

Title	Multi-Layer Polymer Light-Emitting Diodes Prepared by Vapor Deposition Polymerization of Polyazomethine Thin Film
Author(s)	Itabashi, Atsushi; Fukushima, Masao; Murata, Hideyuki
Citation	Japanese Journal of Applied Physics, 47(2): 1271- 1275
Issue Date	2008-02-15
Type	Journal Article
Text version	author
URL	http://hdl.handle.net/10119/7934
Rights	This is the author's version of the work. It is posted here by permission of The Japan Society of Applied Physics. Copyright (C) 2008 The Japan Society of Applied Physics. Atsushi Itabashi, Masao Fukushima, Hideyuki Murata, Japanese Journal of Applied Physics, 47(2), 2008, 1271- 1275. http://jjap.ipap.jp/link?JJAP/47/1271/
Description	

Multi-Layer Polymer Light-Emitting Diodes Prepared by Vapor Deposition

Polymerization of Polyazomethine Thin Film

Atsushi Itabashi¹, Masao Fukushima¹ and Hideyuki Murata^{1,2}

1. School of Materials Science, Japan Advanced Institute of Science and

Technology, Nomi, Ishikawa 923-1292, Japan

2. PRESTO, Japan Science and Technology Agency, Kawaguchi, Saitama 332-0012,

Japan

A novel polyazomethine (PAM) thin film deposited by vapor deposition polymerization (VDP) process was used in the emissive layer of polymer light-emitting diodes (PLEDs). 1,4-bis(4-formylstyryl)benzene (BFSB) and 4,4''-diamino-(1,1',4',1'')-terphenyl (DAT) were co-deposited to form PAM thin films at various substrate temperatures. Fluorescent quantum yield of novel PAM synthesized by using BFSB monomer increased one order of magnitude compared with the previous report. PLEDs with the device structure of ITO / PEDOT:PSS (100 nm) / PAM (140 nm) / LiF (0.5 nm) / Al (80 nm) exhibited of electroluminescence from the PAM layer for the first time. The characteristics of PLEDs suggest the electron mobility of PAM is higher than hole mobility.

KEYWORDS: vapor deposition polymerization; polymer light-emitting diodes, polyazomethine, low annealing temperature, π -conjugated polymer

1. Introduction

Since the discovery of electroluminescence in conjugated polymers by Burroughes *et al.*,¹⁾ polymer light-emitting diodes (PLEDs) have reached the point of application, such as in full-color flat panel displays. There are many issues to be overcome for manufacturing for practical application. In particular, one of the most important problems is lifetime of PLEDs. Light-emitting polymers such as poly(*p*-phenylenevinylene) (PPV) are synthesized by wet process. This process is convenient and low-cost process, but it has some disadvantages. For example, solvents and atmospheric water can not be completely removed from polymer films. These impurities can be one of the reasons for degradation of PLEDs. Recently, our group reported the degradation of OLED by residual water during device fabrication.²⁾

Vapor deposition polymerization (VDP) allows us to form conjugated polymer film on a substrate by direct deposition of monomers. This is a solvent-free process, so we can minimize the impurities in polymer films. Furthermore, the VDP process is suitable for fabrication of multi-layer structure. High efficiency is expected by the employment of multi-layer structure for PLEDs. The advantages of the vapor deposition process over solution-based techniques include good control of film uniformity and thickness. In addition, if the polymer becomes insoluble after film formation, photolithography technique can be used for patterning of the polymer layer.³⁾

The thin films of PPV and polyoxadiazole (POD) have been fabricated with the VDP method.⁴⁻⁷⁾ These materials are synthesized by a two-step reaction process such that precursor polymer forms by polymerization of monomer, and then converts to the final products by heating above 200 °C, typically close to 300 °C. After the conversion, PPV and POD are insoluble for any organic solvents. Applications of PPV⁵⁾ and POD^{6,7)} thin films prepared by VDP for active layer of PLEDs have been reported. Contrary to

PPV and POD, thin films of polyazomethine (PAM) can be prepared by one-step reaction process, with substrate temperature below 200 °C. Such a low-temperature process allows us to use plastic substrates. Application of PAM films for organic light-emitting diodes (OLEDs) has been demonstrated previously.⁸⁻¹⁰⁾ However, these reports only used PAM films as carrier transporting layers of OLEDs. The electroluminescence from PAM prepared by VDP process has never been reported. In this paper, we report successful fabrication of PAM light-emitting devices by VDP process.

2. Experimental

A novel PAM was synthesized by the condensation reaction of 1,4-bis(4-formylstyryl)benzene (BFSB) and 4,4''-diamino-(1,1',4',1'')-terphenyl (DAT), as shown in Fig.1. BFSB and DAT were purchased from Dojindo Laboratory and Lancaster Synthesis Ltd., and used after purification by train sublimation at least two times. The films of PAM were grown by co-evaporation of BFSB and DAT on precleaned silica substrates under the pressure of 10^{-5} Pa. The molar ratio of BFSB to DAT was adjusted to 1 : 1 by controlling evaporation rate of each monomer. The evaporation rate of each monomer was monitored with a quartz crystal microbalance thickness monitor.

UV-vis. absorption and photoluminescence (PL) spectra were measured with a JASCO V-570 spectrophotometer and a FP-6500 fluorophotometer. Absolute PL quantum yield was measured with absolute PL quantum yield measurement system (HAMAMATSU Photonics C9920-02). Infra-red (IR) spectra were measured with a Thermo Nicolet Avatar 360 FT-IR Spectrometer.

Four types of device structures were fabricated on a glass substrate coated with

indium-tin oxide (ITO). In all devices, ITO was used as the anode. LiF/Al was used as the cathode for Devices 1 and 2, and Ca was used for Device 3 and 4.

(1) ITO/PEDOT:PSS/PAM/LiF/Al

(2) ITO/PAM/BCP:PBD/LiF/Al

(3) ITO/PEDOT:PSS/MEH-PPV/Ca/Al

(4) ITO/PEDOT:PSS/MEH-PPV/PAM/Ca/Al

The device structure of Device 1 was ITO/PEDOT:PSS (100 nm)/PAM (140 nm)/LiF (0.5 nm)/Al (80 nm), where PEDOT:PSS stands for poly(3,4-ethylenedioxythiophene) doped with poly(styrenesulfonic acid). An EL grade of PEDOT:PSS (BAYTRON P VP CH8000) was purchased from H. C. Starck Ltd. and used without further purification. First, PEDOT:PSS layer was spin-coated on a pre-cleaned ITO substrate and annealed at 120 °C for 10 min in air. The substrate was set in a vacuum chamber for the growth of PAM thin film. After the deposition of PAM layer at certain substrate temperature (115 °C), deposition of LiF/Al cathode completed device fabrication. Then device was transferred to a nitrogen-filled glove box connected to the growth chamber through a gate valve. The device was encapsulated in the glove box and was subject to device characterization.

The structure of Device 2 was ITO/PAM (140 nm)/BCP:PBD (50 nm)/LiF(0.5 nm)/Al (80 nm). Bathocuproine (BCP) and 2-(4-biphenyl)-5-(4-tert-butylphenyl)-1,3,4-oxadiazole (PBD) were used for electron transport layer (ETL). BCP was kindly provided by Nippon Steel Chemical Co., Ltd., and PBD was purchased from Tokyo Kasei Kogyo Co., Ltd. The BCP:PBD composite thin film was prepared by co-deposition of BCP and PBD.¹¹⁾ LiF/Al was deposited as the cathode. The device was encapsulated in the glove box.

The structure of Device 3 was ITO/PEDOT:PSS (100 nm)/MEH-PPV (200

nm)/Ca (50 nm)/Al (100 nm) where MEH-PPV stands for poly(2-methoxy,5-(2'-ethoxy-hexoxy)-1,4-phenylenevinylene). MEH-PPV was purchased from Aldrich and used without further purification. Chlorobenzene solution of MEH-PPV was spin-coated onto the PEDOT:PSS layer and annealed at 50 °C for 5 hours in a nitrogen glove box. Ca was deposited as a cathode, Al was deposited as a capping protective layer. The device was encapsulated in the glove box.

The structure of Deice 4 was ITO/PEDOT:PSS (100 nm)/MEH-PPV (200 nm)/PAM (45 nm)/Ca (50 nm)/Al (100 nm). Until the formation of MEH-PPV layer, the Device 4 was fabricated at the same way as the Device 3. PAM layer was deposited onto the MEH-PPV layer, and then Ca was deposited as a cathode. Al was deposited as a capping protective layer. The device was encapsulated in the glove box.

Current density (J) -Voltage (V) – Luminance (L) characteristics were measured with a Keithley 4200SCS semiconductor characterization system. Light output from the device was measured with calibrated silicon photodiode mounted on an integrating sphere. The external quantum efficiency (η_{ext}) of EL device was calculated by the method of total luminous flux measurement.¹²⁾

The ionization potential for PAM was measured by photoelectron spectroscopy in air (Riken Keiki, AC-2), and electron affinity level was estimated by subtracting optical gap energy from ionization potential.

3. Results and Discussion

3.1 Absorption and PL spectra of PAM films

Figure 2(a) shows the UV-vis. absorption spectra of PAM films. The monomers were deposited on a substrate at 25 °C and then substrate was transferred to a

nitrogen-filled glove box. The substrate annealed for one hour at various temperatures of 120 °C, 150 °C, 180 °C, 210 °C, 240 °C, 270 °C and 300 °C. The absorption peak shifted with increasing annealing temperature. At the same time, PL intensity increased with increasing annealing temperature (Fig. 2(c)). These results indicate that polymerization took place with increasing annealing temperature. The spectrum of the film annealed at 300 °C showed a strong absorption peak at approximately 525 nm. This is attributed to Mie-scattering effect. By using integrating sphere to remove scattering effect, we obtained the real absorption spectrum of PAM film (Fig. 2(b)). There was no sharp absorption peak at 525 nm in the spectra measured with an integrating sphere. The shift of absorption peak saturates at 180 °C, and the absorption intensity increases slightly with further increases in annealing temperature up to 300 °C. However, the PL intensity was doubled from 180 °C to 300 °C. These results suggest that the conjugation length of PAM does not change at higher temperature, but the amount of conjugated units certainly increased at higher temperature.

Figure 3(b) shows UV-vis. absorption spectra of dichloromethane monomer solutions (BFSB and DAT) and thin film of PAM. The absorption spectra of PAM films were measured with an integrating sphere attached to the spectrometer. DAT and BFSB show sharp absorption at 310 nm and 390 nm. The film of PAM shows broad absorption peaks at 445 and 475 nm. The red-shift of the absorption peak of PAM polymer clearly indicates the extended π -conjugation.

Figure 3(a) shows the DFT calculation of the excited state energies of oligo-phenylenevinylene as a function of number of phenylenevinylene (PV) units.¹³⁾ There is good agreement between the experimental results (Fig. 3(b)) and the theoretical calculation (Fig. 3(a)) of BFSB with two PV repeating units. According to the calculation, it was estimated that optical gap energy of PAM polymer chain could be

equal to five PV repeating units. The five PV units are slightly longer than the length of one component of PAM, where both ends of BFSB monomer were bridged by the phenyl ring of DAT via azomethine group. The conjugating length may be limited by the torsion angle between the phenyl groups in DAT monomer unit.¹⁴⁾ The PAM thin films exhibit green photoluminescence at around 525 nm. The PL quantum yield was 2 % at the excitation wavelength of 350 nm. This PL yield is one order of magnitude higher than that of PAM reported by Weaver *et al.* A typical structure of PAM prepared from *p*-phenylenediamine (PPDA) and terephthalaldehyde (TPA) monomers shows low fluorescent quantum yield (0.2 %). The enhancement of PL yield can be attributed to the chemical structure of PAM, which contains highly fluorescent moiety, two PV units, was incorporated.

3.2 Infrared spectra of PAM films

Two methods were used in polymerization of PAM film. In the first case, the monomers were deposited at 25 °C on the substrate, and then annealed at various temperatures such as 150 °C, 180 °C and 210 °C. Figure 4 shows IR spectra of monomer and PAM films. The strong absorption peaks at 3360 and 1690 cm⁻¹ were assigned to N-H and C=O stretching modes of the amino group and aldehyde group, respectively. We confirmed the progress of polymerization by the decrease in the absorption of monomers. The formation of azomethine bond was confirmed by the appearance of characteristic absorption of azomethine. Figure 5(c) shows a peak separation by using a Gauss fitting at around 1600 cm⁻¹. In general, the peak position of C=N stretching mode of azomethine has been observed at approximately 1600 cm⁻¹.¹⁵⁾ Thus, the characteristics absorption appeared at 1585 cm⁻¹ was assigned to C=N stretching mode of azomethine. An annealing temperature of more than 200 °C was

necessary to prepare PAM film by this method.

In the second case, we polymerized the PAM film by directly depositing monomers on a heated substrate. Figures 5(a) and 5(b) show IR spectra of PAM films which were prepared by different methods. PAM film was produced at low substrate temperature (115 °C) by heating the substrate during monomer deposition. The shift of absorption peak started at 120 °C in the first case (Fig. 2(b)). In each case, chemical reaction started about 120 °C. In the second case, unreacted monomers can leave from substrate by heating substrate. Finally, we can be obtained polymer film with a few residual monomers.

3.3 Polymer light-emitting devices using PAM

Polymer light-emitting devices using PAM as an emitting layer were fabricated. Inset of Fig. 6(b) shows the EL & PL spectra, EL spectrum agrees well with PL spectrum indicates that PAM emits light. This is the first demonstration that PLEDs exhibited of electroluminescence from the PAM layer. The electroluminescence from PAM layer can be attributed to the PL quantum efficiency of PAM, which was 2 % at the excitation wavelength of 350 nm. The maximum external quantum efficiency of EL device¹²⁾ can be estimated to 0.1 % by taking into account PL quantum efficiency (2 %).

Figure 6(a) shows the J-V-L characteristics of multilayer EL devices with different device structures. Threshold voltage of charge injection was 1.6 V. There was no difference at the threshold voltages of charge injection in the two different devices. However, the threshold voltage for light emission of Device 1 was significantly lower than that of Device 2. Maximum external quantum efficiency of Device 1 was 0.0069 %, whereas the device with BCP:PBD as an electron transport layer (ETL) showed lower maximum external quantum efficiency (0.0031 %). Considering these results, PAM film

acts as an n-type polymer. There are two possible reasons for why PAM exhibits n-type character. The first is that the energy barrier of electron injection in PAM is substantially lower than that of hole injection. The second is that electron mobility of PAM is higher than that of hole mobility. The ionization potential for PAM lays in the range from 5.6 to 5.8 eV, and yields a corresponding electron affinity level in the range from 3.2 to 3.4 eV, by subtracting optical gap energy of 2.4 eV. Using typical ionization potentials of PEDOT:PSS (5.5 eV) and LiF/Al (3.2 eV), injection energy barrier of hole injection in PAM was estimated to be 0.1 - 0.3 eV. On the other hand, contact for electron injection between LiF/Al and PAM would be ohmic. Numerical simulations by different groups¹⁶⁾ suggest that an ohmic contact should be formed when the energy barrier at the interface is around 0.3 eV or less, and therefore we considered that ohmic contact would be formed at both PEDOT:PSS/PAM and PAM/cathode interfaces. This situation ruled out the first reason for why PAM exhibits n-type character. We conclude that electron mobility of PAM is higher than hole mobility of PAM. This was supported by electrochemical doping studies for series of chemically coupled polyazomethines.¹⁷⁾

The results of multi-layer polymer LED imply the electron mobility of PAM is higher than hole mobility. An MEH-PPV film is known as a material with higher hole mobility than electron mobility due to electron trap.¹⁸⁾ Thus, in an MEH-PPV single layer device (Device 3), carrier recombination occurs at the cathode interface in the low current density region. The excitons which are generated near the cathode interface are easily quenched by the metal of cathode. Thus, external quantum efficiency of single layer device was low at low current density (Fig. 7(b)). In the high current density region, electron trap might be filled by electron and then carrier recombination may take place at the PEDOT/MEH-PPV interface. In a multi-layer device using PAM as an ETL (Device 4), external quantum efficiency in the low current density area was

improved (Fig. 7(b)). In this device, carrier recombination may occur at MEH-PPV/PAM interface.

4. Conclusion

Thin films of PAM were prepared by VDP process of BFSB and DAT. This PAM film acted as emissive layer in the OLEDs. We have successfully fabricated PLEDs with VDP process. This suggests that the PAM thin film prepared by VDP process could be a promising material for developing PLEDs.

References

- 1) H. Burroughes, D. D. C. Bradley, A. R. Brown, R. N. Marks, K. Macay, R. H. Friend, P. L. Burns and A. B. Holmes: *Nature* **347** (1990) 539.
- 2) T. Ikeda, H. Murata, Y. Kinoshita, J. Shike, Y. Ikeda and M. Kitano: *Chem. Phys. Lett.* **426** (2006) 111.
- 3) K. M. Vaeth and K. F. Jensen: *Adv. Mater.* **11** (1999) 814.
- 4) K. M. Vaeth and K. F. Jensen: *Adv. Mater.* **9** (1997) 490.
- 5) K. M. Vaeth and K. F. Jensen, *Appl. Phys. Lett.* **71** (1997) 2091.
- 6) H. Murata, S. Ukishima, H. Hirano and T. Yamanaka, *Polym. Adv. Technol.* **8** (1997) 459.
- 7) H. Murata: *Synth. Met.* **121** (2001) 1679.
- 8) W. Fischer, F. Stelzer and F. Meghdadi and G. Leising: *Synth. Met.* **76** (1996) 201.
- 9) M. S. Weaver and D. D. C. Bradley: *Synth. Met.* **83** (1996) 61.
- 10) X. Wang, K. Ogino, K. Tanaka and H. Usui: *Thin Solid Films* **438-439** (2003) 75.
- 11) T. Mori and Y. Masumoto: *J. Photopolym. Sci. Technol.* **19** (2006) 209.
- 12) S. R. Forrest, D. D. C. Bradley and M. E. Thompson: *Adv. Mater.* **15** (2003) 1043.
- 13) K. Y. Jen-Shang, C. Wei-Chen and Y. Chin-Hui: *J. Phys. Chem. A* **107** (2003) 4268.
- 14) M. Rumi and G. Zerbi: *Chem. Phys.* **242** (1999) 123.
- 15) C. J. Yang and S. A. Jenekhe: *Macromolecules* **28** (1995) 1180.
- 16) G. G. Malliaras and J. C. Scott: *J. Appl. Phys.* **85** (1999) 7436.
- 17) T. Yamamoto, K. Sugiyama, T. Kushida, T. Inoue and T. Kanbara: *J. Am. Chem. Soc.* **118** (1996) 3930.
- 18) P. W. M. Blom, M. J. M. de Jong and J. J. M. Vleggaar: *Appl. Phys. Lett.* **68** (1996) 3308.

Figure Captions

Fig. 1. Reaction scheme of PAM by vapor deposition of monomers, BFSB and DAT.

Fig. 2. UV-vis. absorption spectra of PAM films measured with (a) transmission mode or (b) reflectance mode using integrating sphere and (c) PL spectra of PAM films. PAM film was deposited at 25 °C, and then annealed at various temperatures such as 120°C, 150 °C, 180 °C, 210 °C, 240 °C, 270 °C and 300 °C.

Fig. 3. (a) DFT calculation of the excited state energies of oligo-phenylenevinylene as a function of number of PV units.¹³⁾ (b) UV-vis. absorption spectra of dichloromethane monomer solutions (BFSB and DAT) and thin film of PAM (300 °C) on silica substrate. The absorption spectra of PAM film was measured with an integrating sphere attached to the spectrometer. PL spectrum of PAM film is shown by broken line.

Fig. 4. FT-IR spectra of monomer and PAM film which were deposited at 25 °C, and then annealed at various temperatures such as 150 °C, 180 °C and 210 °C.

Fig. 5. FT-IR spectra of (a) PAM films deposited at 25 °C, then annealed at various temperatures such as 150 °C, 180 °C and 210 °C. (b) PAM film directly polymerized on a heated substrate in the vacuum chamber. (c) Absorption peak at around 1600 cm⁻¹ was separated by using a Gauss fitting.

Fig. 6. (a) J-V-L characteristics of PLEDs using PAM as an emitting layer and (b) η_{ext} as a function of current density. Inset shows PL spectrum (dotted line) of PAM film and EL spectrum (solid line) from Device 1.

Fig. 7. (a) J-V-L characteristics of PLEDs with or without PAM as an ETL and (b) η_{ext} as a function of current density.

Table I. Assignment of the IR peaks.

ν (cm ⁻¹)	assignment
3360	N-H stretch
1690	C=O stretch
1585	C=N stretch

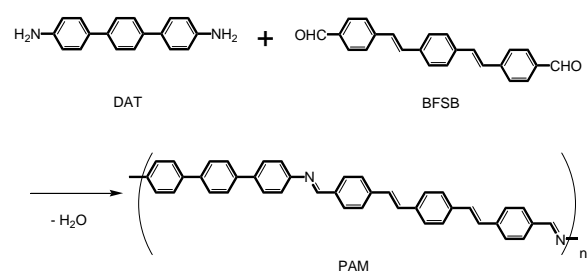


Fig. 1.
A. Itabashi et al.

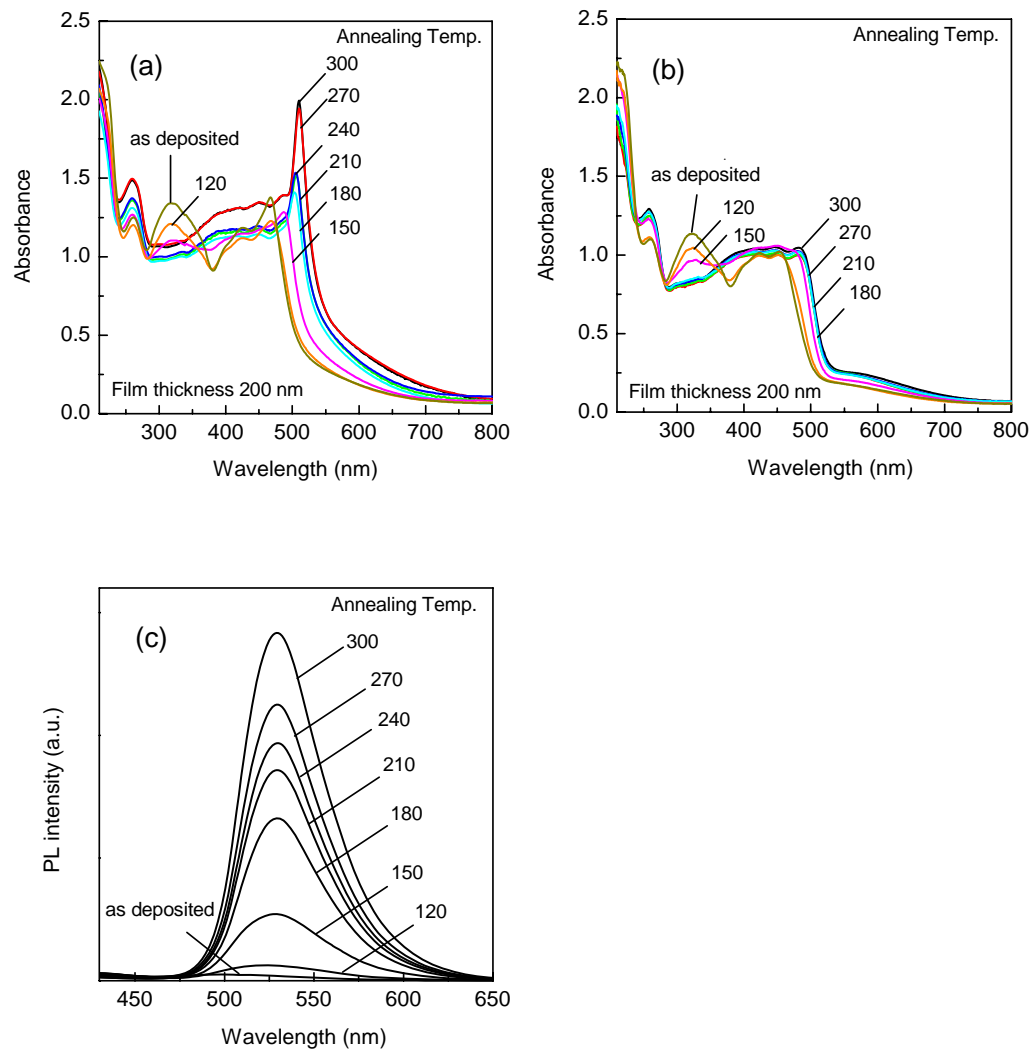


Fig. 2.
A. Itabashi et al.

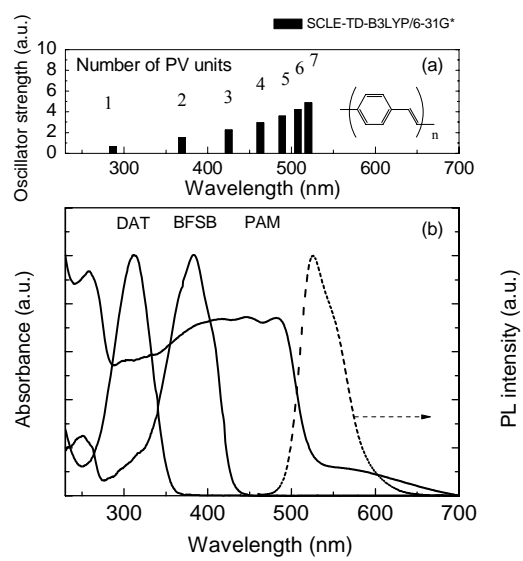


Fig. 3.
A. Itabashi et al.

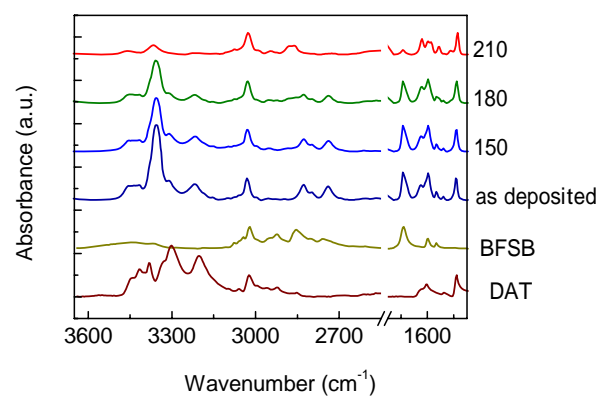


Fig. 4.
A. Itabashi et al.

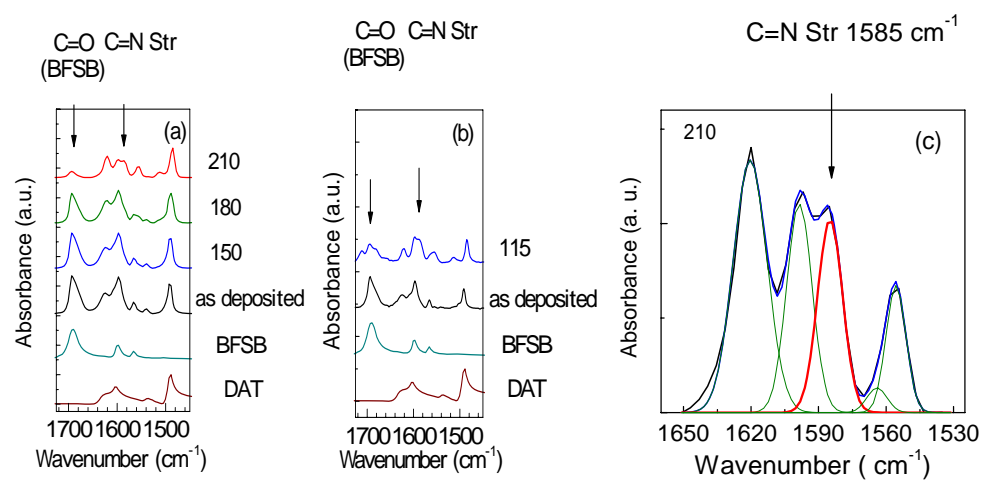


Fig. 5.
A. Itabashi et al.

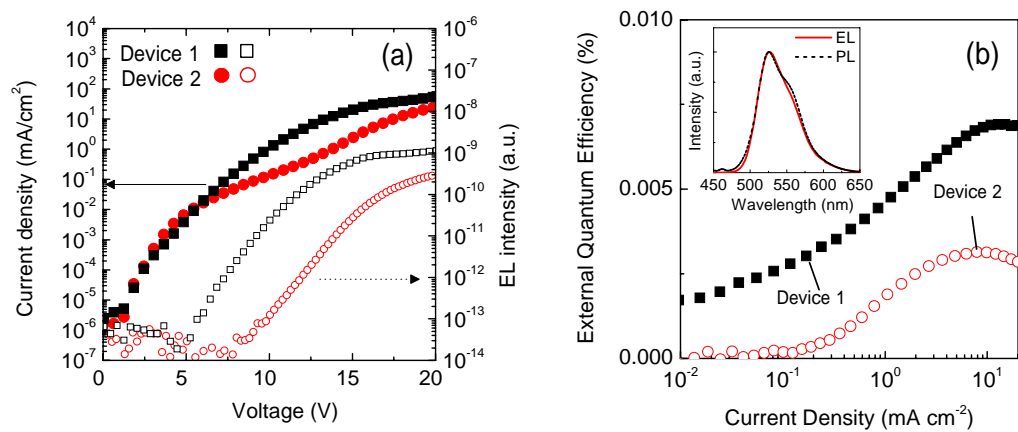


Fig. 6.
A. Itabashi et al.

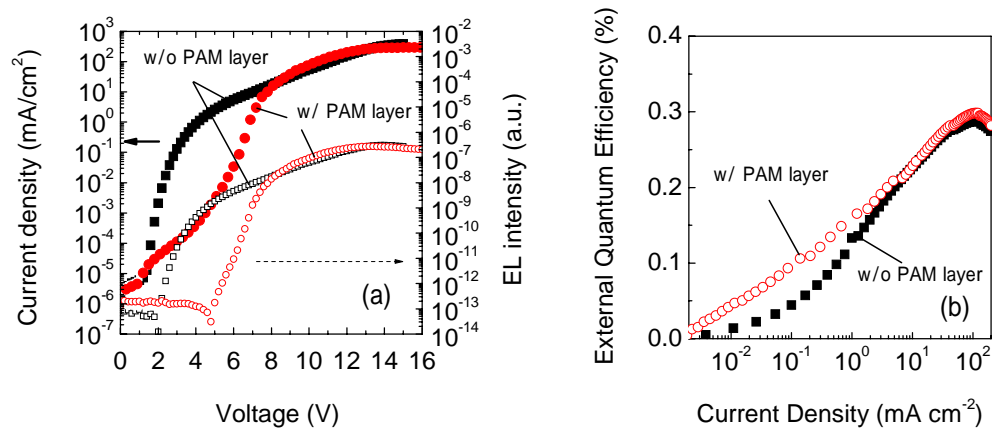


Fig. 7.
A. Itabashi et al.